IOP | Institute of Physics
Computational Physics Group

Newsletter

Theoretical Investigation of Solid Hydrogen and Deuterium
(image courtesy of Dr. Ioan-Bogdan Magdău)

Newsletter Contents

This Newsletter...

Dear Readers,

The feature article for this bumper edition of the newsletter is an invited contribution by Dr Ioan-Bogdan Magdău from the Edinburgh University, the winner of the 2017 IoP Computational Physics Group PhD Prize, on *'Theoretical Investigation of Solid Hydrogen and Deuterium'*.

We also have another feature article entitled *'Electron and Nuclear Dynamics Following Molecular Ionization: Computational Methods and Applications'* provided by one of the runners-up 2017 Dr Morgane Vacher, Imperial College London. Dr Ioan-Bogdan Magdău also kindly provided the cover image for this edition.

Most URLs in the newsletter have web hyperlinks and clicking on them should take you to the corresponding page. The current edition of the newsletter can be found online at:

`www.iop.org/activity/groups/subject/comp/news/page_40572.html`

with previous editions at:

`www.iop.org/activity/groups/subject/comp/news/archive/page_53142.html`

The IoP CPG are also pleased to announce the creation of a new group blog, which can be accessed online at `compphysics.org`. We would advise you to follow the blog for up-to-date information about events and news items. Suggestions for posts can be send via the blogs contact page, compphysics.org/contact.

Enjoy this edition!

Marco Pinna, Newsletter Editor ✉ mpinna@lincoln.ac.uk

(on behalf of the The Computational Physics Group Committee).

Theoretical Investigation of Solid Hydrogen and Deuterium

Dr. Ioan-Bogdan Magdău
Prof. Graeme Ackland

Introduction

Solid hydrogen forms at extreme conditions, under high pressures. The hydrogen atom on its own can be easily tackled analytically and it constitutes a standard textbook problem. In the condensed phase, however, hydrogen becomes surprisingly intricate and it exhibits exceptionally rich physics. At sufficiently high pressures, solid hydrogen has been predicted to become metallic and even a room temperature superconductor. Although the metallic phase remains elusive, numerous other phases have been identified experimentally so far. Understanding the nature of these phases has proven challenging because the conventional methods for determining crystal structure, like X-ray and neutron diffraction are thus far inaccessible at such high pressures. Therefore, our knowledge about the structure of these solid phases comes primarily from theoretical structure predictions followed by validation against the experimentally accessible infrared and Raman spectra. In my PhD work I developed new computational tools to bridge the gap between theory and experiment by simulating the spectra of hydrogen and hydrogen-deuterium mixtures at the precise conditions at which experimental measurements are available. Additionally, I devised a simple thermodynamic model that captures the essential physics of the entire phase diagram, offering a unique perspective to solid hydrogen at extreme conditions. Using these tools I unveiled a possible dynamic interpretation of the recently discovered phase IV of pure hydrogen [1, 2, 3, 4], found evidence for phonon localisation based on mass disorder in hydrogen-deuterium mixtures [5, 6] and showed that, in essence, the phase diagram can be described by a simple close-packing model [7, 8, 9]. The *ab initio* part of our studies was performed using CASTEP [10, 11], while our novel computational tools and methods offered original ways of analysing and interpreting the data.

Raman Spectra from Molecular Dynamics (MD)

Five different solid phases have been confirmed experimentally so far and theory has predicted numerous competing crystal candidates. Especially interesting is the recently discovered solid phase IV which is stabilised by entropy and only exists at high temperatures. Groundbreaking studies employing *ab initio* random structure searching (AIRSS) [12, 13] proposed a surprisingly complicated phase IV crystal candidate with Pc symmetry, shown in figure 1. This structure is comprised of two molecular layer types: a bromine-like (B) layer with compact hydrogen molecules, and a graphene-like (G) layer where the molecules are elongated and organized in molecular trimers forming hexagonal shapes. The stacking is BGBG.
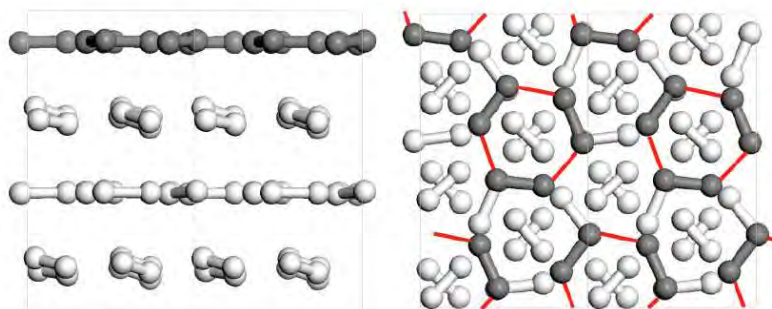

Figure 1: Crystal structure candidate of phase IV (Pc) side and top, reproduced from [13]. The G-layer is shown in dark colour.

Density functional perturbation theory (DFPT) which is routinely used to simulate Raman spectra at zero temperature predicts two distinct vibrational modes ν_1 and ν_2, in agreement with experimental findings. The mode originating

in the B-layer (v_2) is harmonic and well reproduced by the zero kelvin calculation, however the softer mode v_1 involving the elongated molecules in the G-layer is underestimated at this level of theory, casting doubt over the static interpretation of phase IV. The disagreement is somewhat expected, because the experimental phase IV is only stable at high temperatures, while the DFPT spectra are computed at zero kelvin on the ground state structure Pc. We developed a new computational protocol which allows us to approximate Raman spectra from molecular dynamics (MD) at finite temperatures [1, 2, 3, 4]. Our original approach can be summarised in four simple steps:

1. run *ab initio* MD at the experimental pressures and temperatures;

2. project the atomic velocities $\vec{v}_l(t)$ onto the normal modes $\vec{\varepsilon}_{l,k}$ computed in the ground state:

$$c_k(t) = \sum_{l=1}^{N} \vec{v}_l(t) \cdot \vec{\varepsilon}_{l,k} \tag{1}$$

where l labels the atoms and k the normal modes;

3. take the Fourier Transform (FT) of the autocorrelation function for each mode;

$$\tilde{c}_k(\omega) = abs\{FFT\langle c_k(0) \cdot c_k(t)\rangle\} \tag{2}$$

4. multiply each peak with the corresponding DFPT Raman intensity and sum over peaks.

Each FT should generate one Gaussian distribution centred at the correct frequency of that mode, as captured by the dynamics, and with the appropriate line-width. This way the total phonon density of states is decomposed into individual contributions from each vibrational motion. Since we know which of the modes are Raman active, we can approximate the spectrum by selectively summing over those respective modes.

It turns out that solid hydrogen presents additional challenges: at high pressures in phase IV the molecules in the B-layer and the trimers in the G-layer can rotate almost freely, which means that eigen-modes calculated in the ground state become irrelevant. Surprisingly, the Raman active vibrons can be still identified as in-phase molecular stretches despite the continuous molecular reorientation. Therefore, we modified our original protocol and instead of projecting the velocities onto the normal modes, we projected them onto the instantaneous bond defining vectors $\vec{R}_l(t)$:

$$c(t) = \sum_{l=1}^{N} \vec{v}_l(t) \cdot \vec{R}_l(t) \tag{3}$$

This observation allowed us to evaluate the change in the Raman vibrons over the full range of pressures available experimentally as shown in figure 2. We found that vibrons computed with our method agree slightly better with the experiment: in particular, the frequency of v_1 is closer to the measured value. We also obtain peak broadenings which compare well with the observations.

The evolution of the spectra with pressure is intimately related to the dynamics of phase IV. On closer inspection of the trajectories, we noticed subtle changes in the dynamical behaviour upon increasing pressure. While molecules in the B-layers rotate almost freely at all pressures, as illustrated by figure 3, the G-layer trimers only rotate at the higher pressures [14, 1]. The onset of trimer rotation causes the G-layers to break symmetry: half of these layers which we label G" support the rotation, while the other half G' acquire higher hexagonal symmetry. This BG'BG" stacking reproduces well the experimental spectra and could be the correct dynamical interpretation of phase IV. In this case, the finite temperature phase IV can be understood as a highly entropic phase, with a shallow potential energy landscape that is extensively explored at room temperature [15].

We also applied our Raman-from-MD method to the previously proposed crystal structure of phase III (C2/c) [12]. Experimentally, the signature of phase III is a single vibron, which is weaker than v_2 of phase IV, but stronger than v_1. As shown in figure 2 the Raman spectra computed with DFPT agree quite well with the measurement, but the change with pressure is slightly different. Our finite temperature method solves the disagreement and reproduces
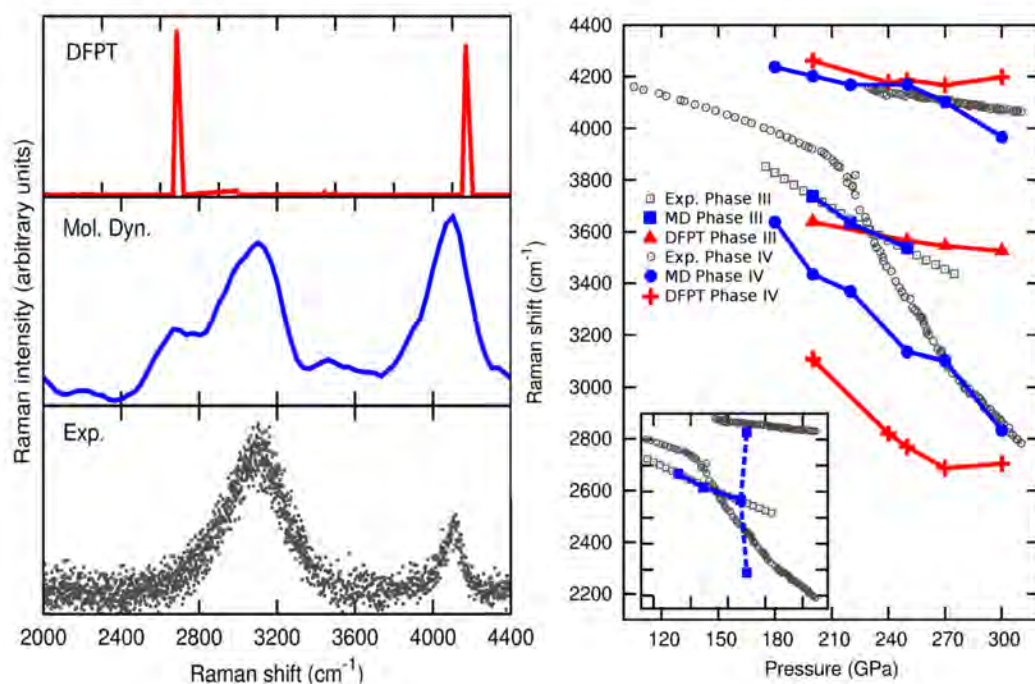
Figure 2: Left: the vibrational spectrum of phase IV at 270 GPa, computed with DFPT at zero kelvin (top), extracted from MD with our method (centre) and measured experimentally (bottom). Right: the frequency of the Raman vibrons in phases III and IV vs pressure, obtained with the three different methods. Inset: upon compression, the simulation started in phase III transforms to phase IV as illustrated by the splitting of the Raman active vibron.
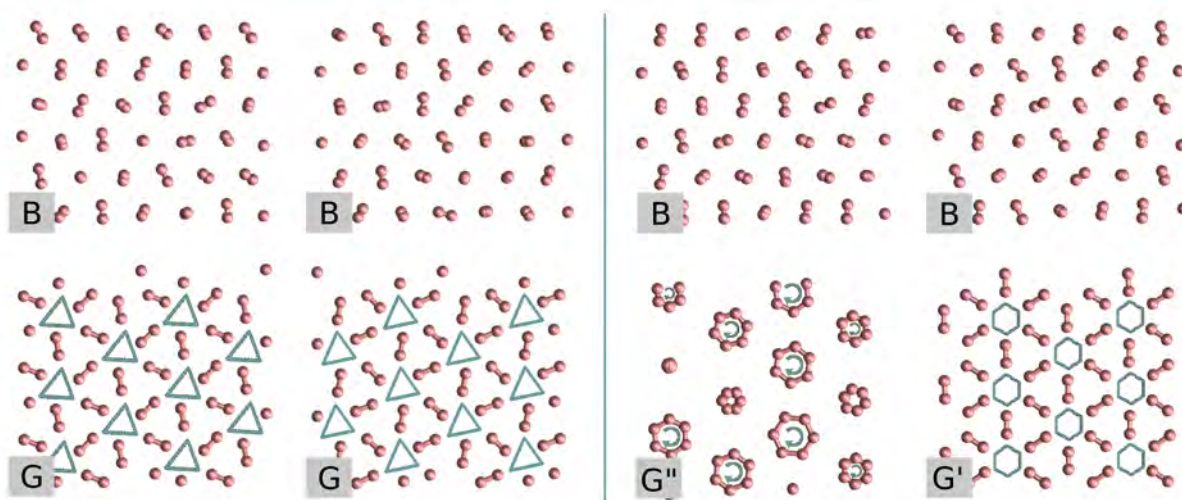
Figure 3: Averaged coordinates over 1 ps of trajectory at 220 GPa (left) and 270 GPa (right). The structures are illustrated layer by layer. Rotating B-layer molecules and G-layer trimers are averaged into a dot.

the measured pressure trend. We visualize the MD trajectories and find that C2/c is better behaved than Pc, and therefore the predicted ground state geometry describes phase III well even at finite temperature. In this case, our method simply corrects for the anharmonicity and inter-molecular coupling of the vibrations. Upon pressurising phase III we observe a transition to phase IV, which is further evidence that our simulations are robust.

Our new high temperature approach for computing spectra helped narrow the gap between previous theoretical and experimental results in phases III and IV. This method is transferable and can be applied to other hydrogen phases

that are only stable at high temperature or which are highly anharmonic. The liquid phase is the next natural candidate and will be considered in future work.

Infrared and Raman Spectra in Hydrogen-Deuterium Mixtures

Isotopic substitution is a powerful experimental tool for investigating the condensed phase. In particular, the deuterium isotope is twice as heavy as hydrogen and this 1:2 mass ratio is the largest of any isotope pair giving rise to considerably large effects in the solid hydrogen phases. Hydrogen-deuterium mixtures have, therefore, attracted a lot of experimental attention recently. Independent measurements performed in phase III [16] and phase IV [5] have found complicated vibrational spectra that were broadened, split and shifted in frequency compared to pure isotopes. These results were difficult to interpret in the absence of any simulation data and in case of phase III had been mistakenly attributed to new solid phases that were thought to be stable in mixtures but not in pure isotopes. Calculating infrared and Raman spectra in hydrogen-deuterium mixtures is not straightforward because the arrangement of the isotopes on the lattice is random which breaks the translational symmetry and the solid becomes non-periodic. I developed a computational method to tackle this problem and was able to calculate the spectra which we found to be in good agreement with the experimental observations [5, 6]. The results gave us a new perspective on the behavior of hydrogen-deuterium mixtures and we now understand the complex spectra are the result of phonon localisation induced by mass disorder and are not the signature of structural phase transitions.

The spectra of mixtures were computed by extensively sampling from a random distribution of isotopic arrangements on the lattice. Our method exploits the fact that hydrogen and deuterium have the same electronic structure so forces felt by the atoms on the Born-Oppenheimer potential energy surface are the same regardless of their isotopic identity. Therefore, the expensive part of a DFPT calculation, namely the Hessian matrix only needs to be performed once. Our protocol follows these steps:

1. compute the Hessian and the Born charges for a unit cell of pure hydrogen;

2. generate a collection of mixture samples $\{s\}$ by randomly assigning atoms on the lattice to either H or D, according to a target concentration c;

3. for every sample s, compute the eigen-modes $\vec{\varepsilon}_{l,k,s}$ and eigen-frequencies $\omega_{k,s}$ at the gamma point by re-diagonalizing the mass-normalized dynamical matrix;

4. compute the infrared intensity for each mode k using the matrix of Born charges $\overline{\overline{B}}_l$, where l labels the atoms (equation 3.113 from [17]):

$$I_{IR}[\omega_{k,s}] = \left(\sum_{l=1}^{N} \overline{\overline{B}}_l \cdot \vec{\varepsilon}_{l,k,s} \right) \cdot \left(\sum_{l=1}^{N} \overline{\overline{B}}_l \cdot \vec{\varepsilon}_{l,k,s} \right)^T \tag{4}$$

5. approximate the Raman intensity for the vibron modes with a variation of the ansatz used for the MD approach:

$$I_{Raman}[\omega_{k,s}] = \sum_{l=1}^{N} \vec{R}_l \cdot \vec{\varepsilon}_{l,k,s} \tag{5}$$

where instead of instantaneous velocities, we projected the normal modes onto the bond defining vectors $\vec{R}_l$. We exploit the same idea that Raman active vibrations are in-phase oscillations;

6. compute phonon localisation as the inverse participation ratio of the atoms to a given mode:

$$L[\omega_{k,s}] = \sum_{l=1}^{N} \left(\vec{\varepsilon}_{l,k,s} \cdot \vec{\varepsilon}_{l,k,s} \right)^2 \tag{6}$$

7. obtain the infrared $I_{IR}[\omega_k]$ and Raman $I_{Raman}[\omega_k]$ spectra and the phonon localisation $L[\omega_k]$ for mixtures as histograms over individual samples s, while checking that the number of mixture configurations is sufficient to ensure convergence.

Calculating Raman from *ab initio* MD at finite temperatures in mixtures is impractical because it requires good sampling of random isotopic arrangements. This could be achieved either by running a large number of trajectories, each with a different isotopic arrangement, or by running a few trajectories with large unit cells to compensate for the lack of translational symmetry. Both approaches are computationally expensive, however for phase IV, where the G-layer vibrons are problematic in DFPT, we did perform one MD simulation with a moderately large unit cell to gauge the effect of the dynamics.
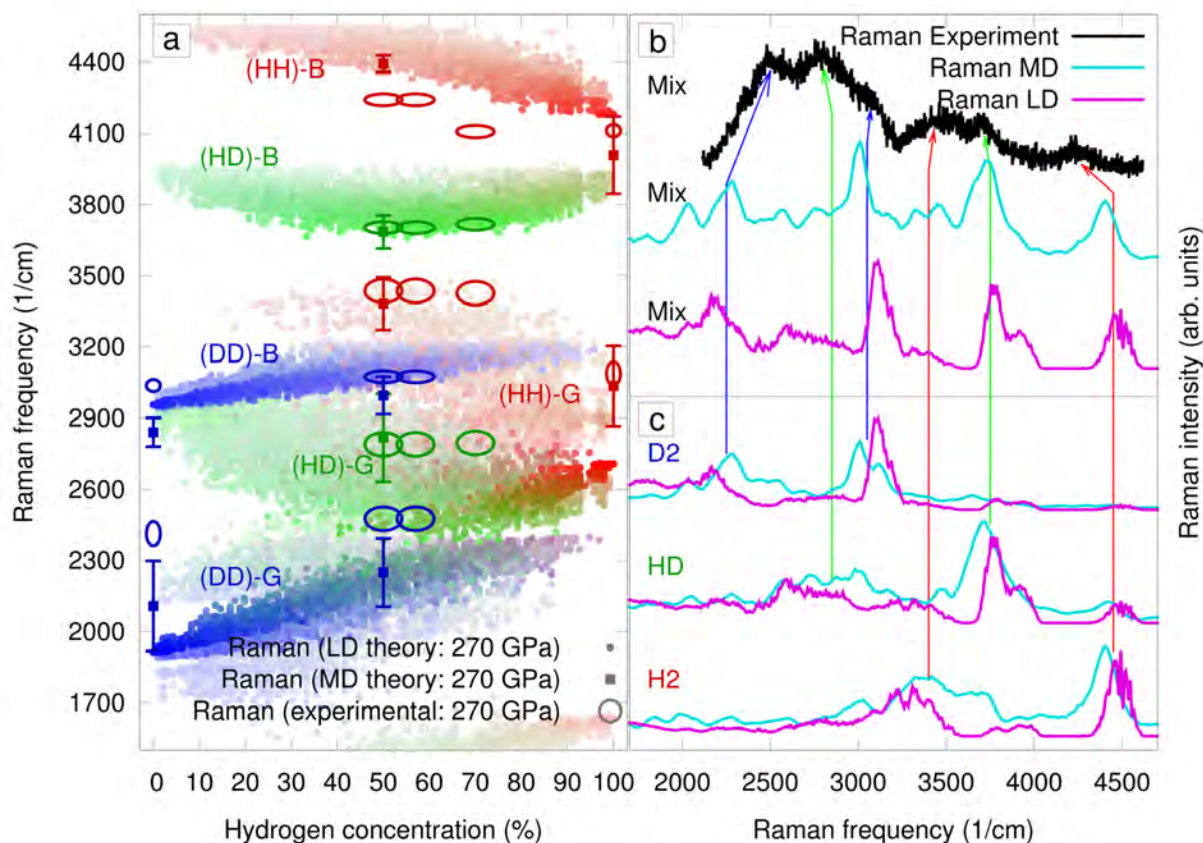

Figure 4: Raman spectra in phase IV of H:D mixtures at 270 GPa and various concentrations. Left: DFPT (or lattice dynamics LD), MD and experimental results. Colours are assigned based on the origin of the peak: HH (red), HD (green) or DD (blue), while the saturation based on their intensity. Right: the full spectrum (top) and contributions from different species (bottom).

Our results for both phases III and IV are in good agreement with experimental measurements. In phase IV, we find six classes of vibrations consistent with the two different layer types and three molecular species: ν_1^{HH}, ν_1^{HD}, ν_1^{DD}, ν_2^{HH}, ν_2^{HD} and ν_2^{DD}. As shown in figure 4 all the vibrons can be separated into these categories and there is little coupling and mixing between them. We understand this through a phenomenon of phonon localisation induced by mass disorder. The large isotopic ratios are sufficient to weaken the coupling between neighbour molecules to the extent that the phonon bands are broken into vibrations localised on a few molecular islands with similar isotopic composition. The trend of the vibrational frequencies with concentration can also be explained by phonon localisation. When any one of the three molecular species occurs at low concentrations in the mixtures, their corresponding vibrations occur at higher frequency and vice versa. The groups of molecules that are coherently involved in a localised vibration stochastically decrease in size as the concentration of that molecular species decreases, driving up

the frequency of those vibrations. Although localisation cannot be directly measured in experiments, we observed that the experimental trend of the frequencies with concentrations is similar, which provides strong indirect evidence for this phenomenon.
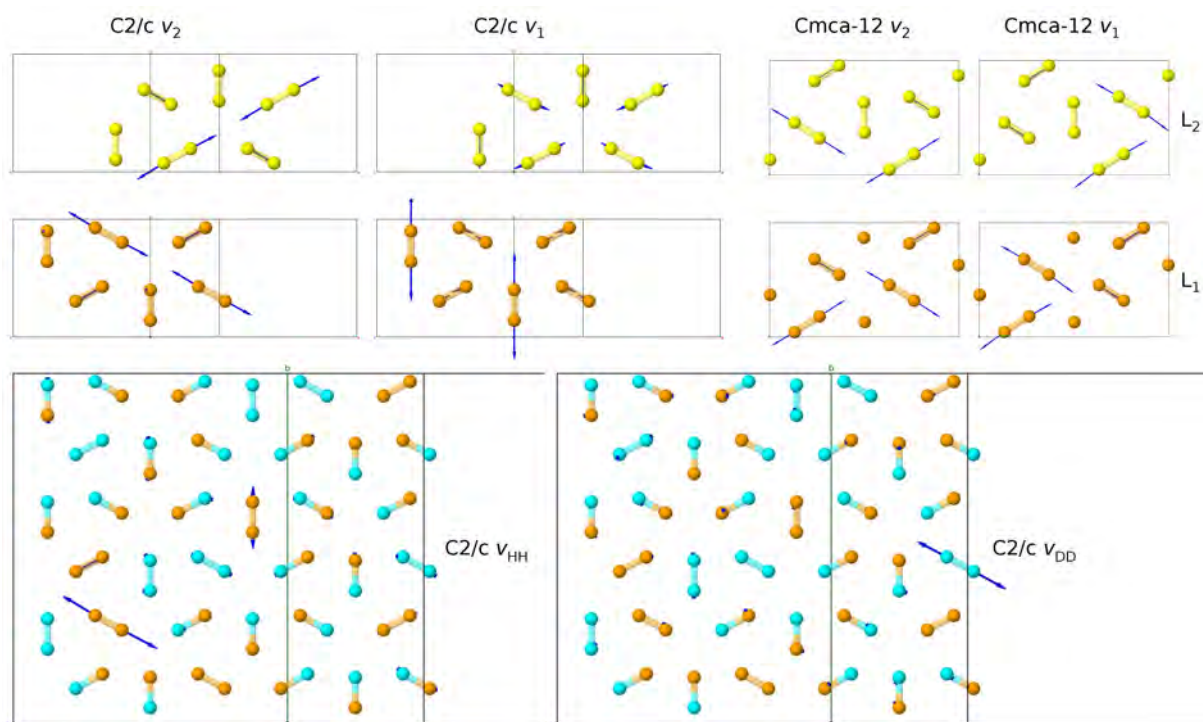

Figure 5: Top: the eigen-modes corresponding to the infrared active vibrations in pure hydrogen, structures C2/c and Cmca-12. The two layers for each unit cell are shown in different colours. Bottom: representative eigen-modes for an infrared active localised vibration in mixtures.

In phase III, we carried out our infrared analysis on the structures C2/c and Cmca-12 which are the best candidates found in AIRSS [12]. Phase III is a stacking of slightly more distorted G-layers and has no B-layers. As illustrated in figure 5, on close inspection of the eigen-modes in mixtures we found similar localisation of the vibrational motions. Surprisingly, in phase III our simulations even capture the splitting of the infrared spectra into multiple sub-peaks, in agreement with the experimental findings [16]. Whereas the experimental study attributes this splitting to a phase transition, we show that it can be understood through phonon localisation. The vibrations are concentrated onto local groups of molecules and the variety of such molecular environments is limited by the symmetry of the crystal structure which results in a subdivision of the peaks into multiple sub-peaks.

Overall, our computational approach for simulating infrared and Raman spectra in H:D mixtures of phases III and IV gave good results which were in agreement with the experiments. We provided evidence to the phenomenon of phonon localisation by mass disorder which had not been observed before. This phenomenon might be specific to H:D mixtures owing to their large 1:2 isotopic mass ratio which is unique amongst the elements.

A Packing Model of the Hydrogen Phase Diagram

Understanding the phase diagram of solid hydrogen and isotopes is a formidable task and many excellent research groups are working on this problem. Recent studies [18, 19, 20] have shown that exchange-correlation and nuclear effects are important contributions to the total energy of the various candidate crystal structures, which makes the *ab initio* computations exceedingly expensive. While these accurate calculations play a crucial role in solving the phase diagram, it is surprising how far we can get with a model based on simple thermodynamics. In my PhD work I formulated an instructive computational model that, based on considerations of close-packing and simple
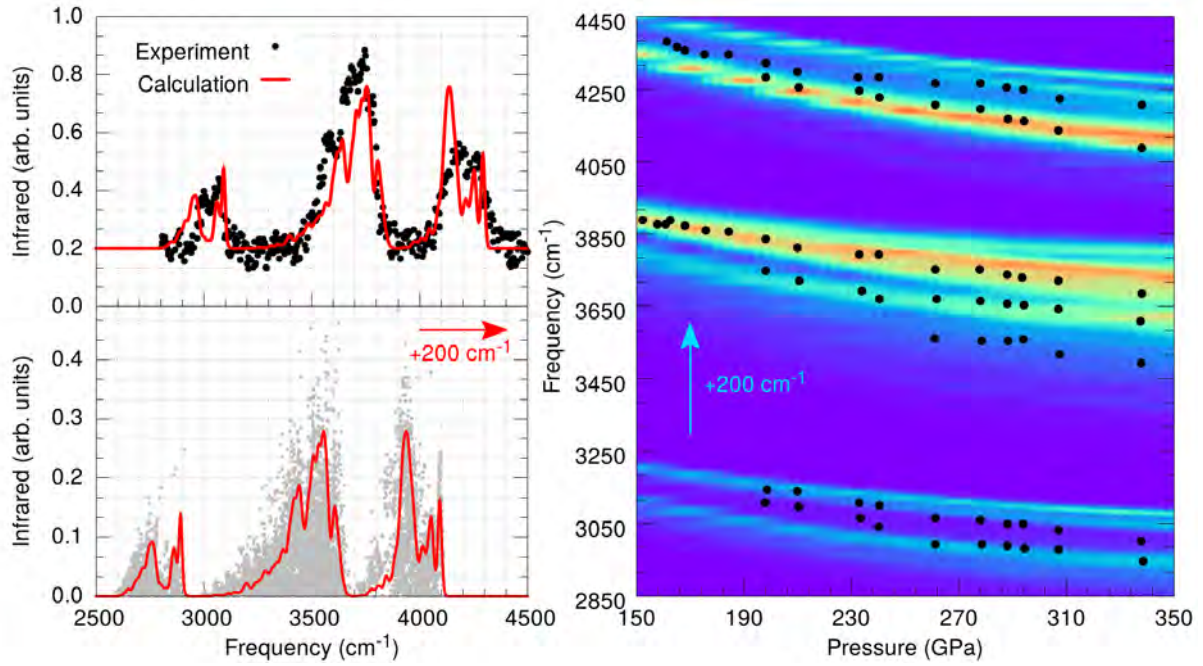
Figure 6: Left: Infrared spectrum computed for phase III at 50:50% H:D mixtures, 300 GPa, experiment and simulation. The theoretical spectra were shifted up in frequency by 200 cm^{-1} to account for finite temperature effects that are not captured in DFPT. Right: infrared spectra as function of pressure, experimental data shown with black dots and simulation as a colour map.

thermodynamics, captures most of the important features of the phase diagram [7, 8, 9]. All of the hypothesis we used in our model were derived from previous *ab initio* studies by ourselves and others. In the following we list the free energies for each phase accompanied by the corresponding underlying assumptions:

1. Solid hydrogen phase I is a hexagonal close-packing of hydrogen rotors, in this simple picture modeled as spheres (S) with an associated bond energy U_S, volume V_S and entropy S_S:

$$G_1(P, T) \approx U_S + \frac{P \times V_S}{c_1} - T \times S_S \tag{7}$$

   c_1 is the packing fraction of hcp;

2. Phase II is the corresponding low-temperature broken symmetry phase comprising of molecules stabilised by quadrupole interactions U_2, here modeled as rods (R) with an internal bond energy $U_R = U_S$ volume V_R smaller than V_S and zero entropy:

$$G_2(P, T) \approx U_2 + U_R + \frac{P \times V_R}{c_2} \tag{8}$$

   c_2 is a packing fraction less efficient than c_1;

3. Likewise, phase III is comprised of R objects with a slightly better packing c_3 but no attractive quadrupole energy:

$$G_3(P, T) \approx U_R + \frac{P \times V_R}{c_3} \tag{9}$$

4. As discussed above, phase IV is dynamic in nature. Figure 7 shows the proton density surfaces extracted from *ab initio* MD trajectories, and the abstract representation of the average symmetry. It is clear that there are two kinds of G-layers, both comprising of two different hexagonal motifs. Our finite temperature analysis shows that at slightly higher pressure there exists a more symmetric phase V, where both G-layers become

fully symmetric and the B-layers continue to freely rotate. The difference between phases IV and V is subtle and cannot be easily captured by our coarse model. We view both phases IV and V as a very efficient packing of spherical objects of different dimensions: atoms (A) in the G-layer and rotors S in the B-layer:

$$G_4(P,T) \approx \frac{U_S}{2} + \frac{P \times (V_A + V_S)}{2c_4} - \frac{T \times S_S}{2} \tag{10}$$

with half the molecules dissociated, the internal energy and entropy are divided by half, V_A is twice the volume of two individual atoms and is smaller than V_R. The packing c_4 is more efficient than c_1;
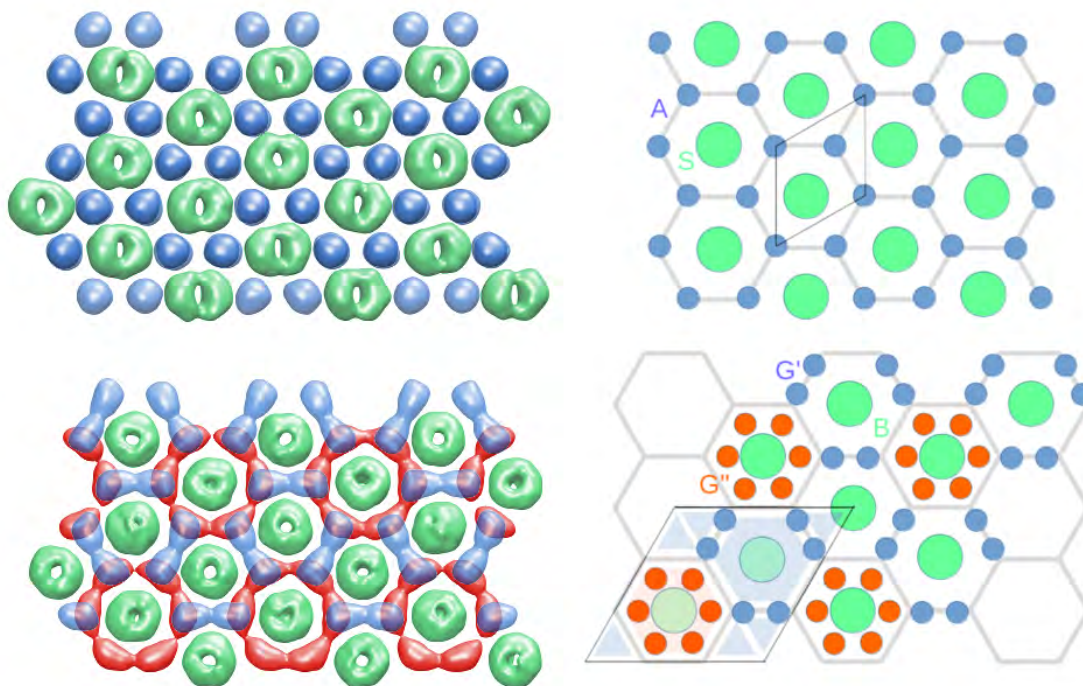

Figure 7: Top/Bottom: phases V/IV. Left: proton density surfaces extracted from *ab initio* MD trajectories. Right: simple interpretation of the phases V and IV, modeled as an efficient packing of spherical rotors (S) and atoms (A). The B layers are shown in green, G layers (phase V) in blue and G'/G" layers (phase IV) in blue/red.

5. Predicted phase VI was modeled here as a simple hexagonal close-packing ($c_5 = c_1$) of atoms (A), with no internal energy and no entropy.

$$G_5(P,T) \approx \frac{P \times V_A}{c_5} \tag{11}$$

6. Finally the liquid is represented as a combined Boltzmann distribution of S, R and A objects. For details check [7].

In addition to the terms listed above, our complete model includes zero point energy as a temperature offset and an assumption for the equation of state [7].

Based on these assumptions and a set of reasonable parameters we computed free energies across a range of pressures and temperatures and were able to reproduce the experimental diagram surprisingly well. We have shown that our simple model successfully captures the underlying thermodynamics of hydrogen at extreme conditions and summarises in a compact way the numerous conclusions drown from state of the art experimental and computational studies by others and ourselves.
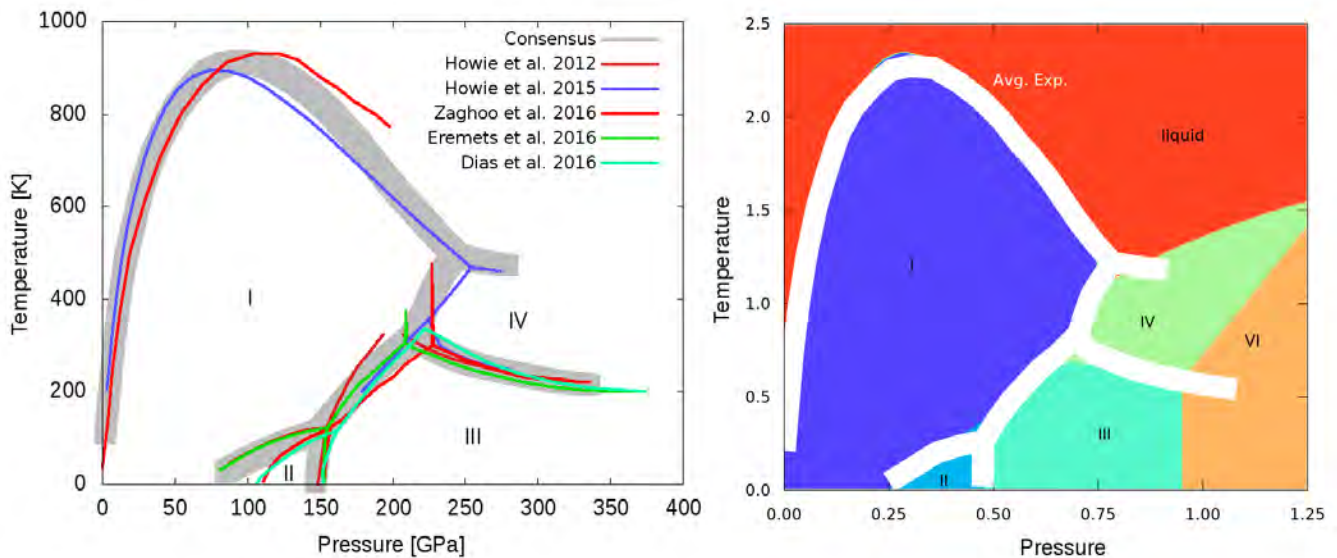
Figure 8: Left: proposed diagrams from recent experiments[21, 22, 23, 24, 25] accompanied by tentative phase borders that reconcile these studies (gray). Right: the theoretical phase diagram derived from our simple packing model as colour map, with the experimental phase boundaries shown in white.

Conclusions

Our first two studies helped improve our understanding of phases III and IV of solid pure hydrogen and hydrogen-deuterium mixtures, respectively. This was achieved by developing novel computational approaches to carry out analysis at the pressure, temperature and concentration conditions explored by experiments. We revealed the finite temperature behaviour of pure hydrogen phase IV and accounted for some of the discrepancies between computed and measured spectra in both phases III and IV. We have uncovered an exciting phenomenon of phonon localisation by mass disorder that could be specific to hydrogen isotopic mixtures and explains the experimental findings. Finally, we have captured the essence of the hydrogen phase diagram in a simple thermodynamic model. This shows how complex and intriguing the emergent behaviour of the simplest element is, when cornered at extreme conditions in its condensed forms.

For in depth details on our studies, I welcome the reader to consult my PhD thesis which is available at https://www.era.lib.ed.ac.u and our previous publications [1, 2, 3, 4, 5, 6, 7, 8, 9].

References

[1] I. B. Magdău and G. J. Ackland, "Identification of high-pressure phases III and IV in hydrogen: Simulating Raman spectra using molecular dynamics," *Physical Review B*, vol. 87, no. 17, p. 174110, 2013.

[2] G. J. Ackland and I. B. Magdău, "Efficacious calculation of Raman spectra in high pressure hydrogen," *High Pressure Research*, vol. 34, no. 2, pp. 198–204, 2014.

[3] I. B. Magdău and G. J. Ackland, "High temperature Raman analysis of hydrogen phase IV from molecular dynamics," in *Journal of Physics: Conference Series*, vol. 500, p. 032012, IOP Publishing, 2014.

[4] G. J. Ackland and I. B. Magdău, "Appraisal of the realistic accuracy of molecular dynamics of high-pressure hydrogen," *Cogent Physics*, vol. 2, no. 1, p. 1049477, 2015.

[5] R. T. Howie, I. B. Magdău, A. F. Goncharov, G. J. Ackland, and E. Gregoryanz, "Phonon localization by mass disorder in dense hydrogen-deuterium binary alloy," *Physical Review Letters*, vol. 113, no. 17, p. 175501, 2014.

[6] I. B. Magdău and G. J. Ackland, "Infrared peak splitting from phonon localization in solid hydrogen," *Physical Review Letters*, vol. 118, no. 14, p. 145701, 2017.

[7] I. B. Magdău, M. Marqués, B. Borgulya, and G. J. Ackland, "Simple thermodynamic model for the hydrogen phase diagram," *Physical Review B*, vol. 95, no. 9, p. 094107, 2017.

[8] I. B. Magdău, F. Balm, and G. J. Ackland, "Thermodynamics and packing in the hydrogen phase diagram," *accepted for publication in Journal of Physics: Conference Series*, 2017.

[9] I. B. Magdău and G. J. Ackland, "Charge density wave in hydrogen at high pressure," *accepted for publication in Journal of Physics: Conference Series*, 2017.

[10] M. D. Segall, P. J. D. Lindan, M. J. Probert, C. J. Pickard, P. J. Hasnip, S. J. Clark, and M. C. Payne, "First-principles simulation: ideas, illustrations and the castep code," *Journal of Physics: Condensed Matter*, vol. 14, no. 11, p. 2717, 2002.

[11] S. J. Clark, M. D. Segall, C. J. Pickard, P. J. Hasnip, M. J. Probert, K. Refson, and M. C. Payne, "First principles methods using castep," *Zeitschrift für Kristallographie-Crystalline Materials*, vol. 220, no. 5/6, pp. 567–570, 2005.

[12] C. J. Pickard and R. J. Needs, "Structure of phase III of solid hydrogen," *Nature Physics*, vol. 3, no. 7, pp. 473–476, 2007.

[13] C. J. Pickard, M. Martinez-Canales, and R. J. Needs, "Density functional theory study of phase IV of solid hydrogen," *Physical Review B*, vol. 85, no. 21, p. 214114, 2012.

[14] H. Liu and Y. Ma, "Proton or deuteron transfer in phase IV of solid hydrogen and deuterium," *Physical Review Letters*, vol. 110, no. 2, p. 025903, 2013.

[15] H. Liu, L. Zhu, W. Cui, and Y. Ma, "Room-temperature structures of solid hydrogen at high pressures," *The Journal of Chemical Physics*, vol. 137, no. 7, p. 074501, 2012.

[16] R. P. Dias, O. Noked, and I. F. Silvera, "New phases and dissociation-recombination of hydrogen deuteride to 3.4 Mbar," *Physical Review Letters*, vol. 116, no. 14, p. 145501, 2016.

[17] P. R. Tulip, *Dielectric and lattice dynamical properties of molecular Crystals via density functional perturbation theory: implementation within a first principles code*. PhD thesis, Durham University, 2004.

[18] M. A. Morales, J. M. McMahon, C. Pierleoni, and D. M. Ceperley, "Nuclear quantum effects and nonlocal exchange-correlation functionals applied to liquid hydrogen at high pressure," *Physical Review Letters*, vol. 110, no. 6, p. 065702, 2013.

[19] J. Chen, X. Ren, X. Z. Li, D. Alfè, and E. Wang, "On the room-temperature phase diagram of high pressure hydrogen: An ab initio molecular dynamics perspective and a diffusion monte carlo study," *The Journal of Chemical Physics*, vol. 141, no. 2, p. 024501, 2014.

[20] N. D. Drummond, B. Monserrat, J. H. Lloyd-Williams, P. L. Ríos, C. J. Pickard, and R. J. Needs, "Quantum monte carlo study of the phase diagram of solid molecular hydrogen at extreme pressures," *Nature Communications*, vol. 6, 2015.

[21] R. T. Howie, T. Scheler, C. L. Guillaume, and E. Gregoryanz, "Proton tunneling in phase IV of hydrogen and deuterium," *Physical Review B*, vol. 86, no. 21, p. 214104, 2012.

[22] R. T. Howie, P. Dalladay-Simpson, and E. Gregoryanz, "Raman spectroscopy of hot hydrogen above 200 GPa," *Nature Materials*, vol. 14, no. 5, pp. 495–499, 2015.

[23] M. Zaghoo, A. Salamat, and I. F. Silvera, "Evidence of a first-order phase transition to metallic hydrogen," *Physical Review B*, vol. 93, no. 15, p. 155128, 2016.

[24] M. I. Eremets, I. A. Troyan, and A. P. Drozdov, "Low temperature phase diagram of hydrogen at pressures up to 380 GPa. A possible metallic phase at 360 GPa and 200 K," *arXiv preprint arXiv:1601.04479*, 2016.

[25] R. Dias, O. Noked, and I. F. Silvera, "New insulating low temperature phase in dense hydrogen: The phase diagram to 421 GPa," *arXiv preprint arXiv:1603.02162*, 2016.

Electron and Nuclear Dynamics Following Molecular Ionization: Computational Methods and Applications

Dr Morgane Vacher Department of Chemistry, Imperial College, London SW7 2AZ, United Kingdom
Department of Chemistry – Ångström, Uppsala University, Uppsala 75121, Sweden

Introduction

Understanding chemical reactions and biological processes ultimately depends upon understanding electronic motion in detail, since it is the collective motion of the electrons that initiates specific rearrangements of atoms in molecules. Because of their light mass, electrons are expected to move on the attosecond (1 as = 10^{-18} s) timescale. The first synthesis of attosecond light pulses in 2001 [1, 2] opened up the possibility to probe electronic motion experimentally on its natural timescale, and potentially to control it. Because of the time-energy uncertainty principle $\Delta E \Delta t \geq \hbar$, such short laser pulses have a broad spectral bandwidth (up to several eV) and lead to the coherent population of several electronic states (Figure 9a). The latter is called an "electronic wavepacket" and is non-stationary, i.e. its probability density is time-dependent. The interference between electronic eigenstates in such a superposition, alternating between constructive and destructive, leads to oscillating motion of the electronic density (Figure 9b). This is "pure" quantum electron dynamics (i.e., takes place even if the nuclei are fixed) and is often called *charge migration* in the literature [3].

Because the electronic distribution is usually considered to be changing much faster than the nuclear geometry, many theoretical studies so far treated molecular electron dynamics upon ionisation as a purely electronic process: by neglecting the nuclear coordinates, long-lived oscillations in the electronic density at a well-defined period (inversely proportional to the energy gap) are then predicted. There has been an enormous experimental effort dedicated to observe the predicted oscillations in the electronic density of molecules [4], unsuccessful so far. But what does the oscillatory electronic motion actually become when the nuclear coordinates are taken into account? My doctoral work has been concerned with fundamental and outstanding questions about the physics of non-stationary electronic wavepackets created upon sudden photoionisation of molecules, in particular the coupling between electronic and nuclear motions.
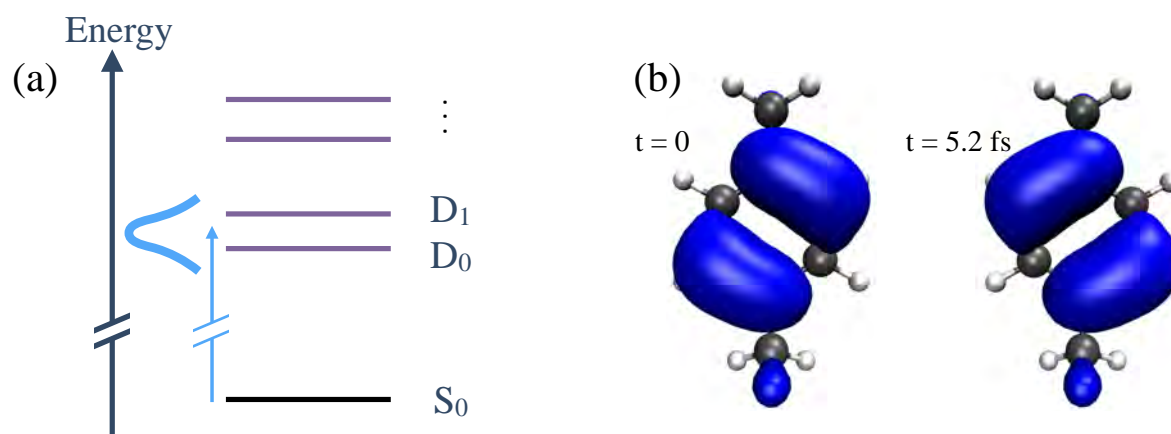

Figure 9: (a) An attosecond pulse leads to the coherent population of several electronic states of the cation because of its large spectral bandwidth. (b) Prediction of long-lived oscillations in the electronic density of para-xylene cation when neglecting the nuclear coordinates [5].

Methods for simulating coupled electron and nuclear dynamics

To describe the electronic and nuclear motions in molecules, one needs to solve the molecular time-dependent Schrödinger equation:

$$i\hbar \frac{\partial}{\partial t}\Phi(\mathbf{r}, \mathbf{R}, t) = \hat{\mathcal{H}}(\mathbf{r}, \mathbf{R})\Phi(\mathbf{r}, \mathbf{R}, t) \tag{12}$$

This equation being impossible to solve analytically for more than two particles, i.e. the hydrogen atom, numerical and approximate methods have been developed to treat other atoms and molecules. Standard quantum mechanical simulations involve numerical integration of equation (12) on grids. The exponential scaling with the system size makes these methods poorly adequate for the study of molecules of reasonable size. A separate bottleneck is the calculation and fitting of the potential energy surfaces before any dynamics calculation. "On-the-fly" or "direct-dynamics" methods address these issues by calculating the potential energy surfaces as needed along nuclear trajectories [6]. The total nuclear wave packet is expanded in the basis of these nuclear trajectories that sample only the relevant regions of the potential energy surfaces. There exist several on-the-fly methods able to describe non-adiabatic dynamics; they differ mainly in the treatment of the nuclear motion (Figure 10). An important distinction is between "multi-set" type of methods where each electronic state has its own set of basis trajectories and "single-set" type of methods where all electronic states share the same set of basis trajectories. We will argue that the latter class is more natural for the simulation of molecular coherent electron dynamics since each nuclear trajectory "feels" all populated electronic states.

During my doctoral work, I have used both a fully quantum mechanical method called direct-dynamics variational multi-configurational Gaussian (DD-vMCG) and an approximate semi-classical method called Ehrenfest method. The former historically comes from the multi-configurational time-dependent Hartree (MCTDH) method, which is an efficient grid-based quantum dynamics method. To remove the restrictions of the grid, the G-MCTDH method was introduced, where some of the multi-dimensional basis functions are replaced by parametrised Gaussian functions. The vMCG method corresponds to the case where only Gaussian functions are included in the G-MCTDH method and its direct dynamics implementation is known as DD-vMCG. So in the DD-vMCG method, the nuclear wave packet is described using a set of Gaussian basis functions (GBF) which evolve quantum mechanically and are variationally coupled while in the Ehrenfest method, the coupling between electronic and nuclear degrees of freedom is treated in a mean-field manner using independent nuclear trajectories which obey classical mechanics [7]. It is noted that there exists intermediate methods between the Ehrenfest method and the DD-vMCG method, which build on Ehrenfest trajectories and couple them together [6, 8]. They differ from the DD-vMCG method since the basis trajectories obey classical and not quantum mechanics.
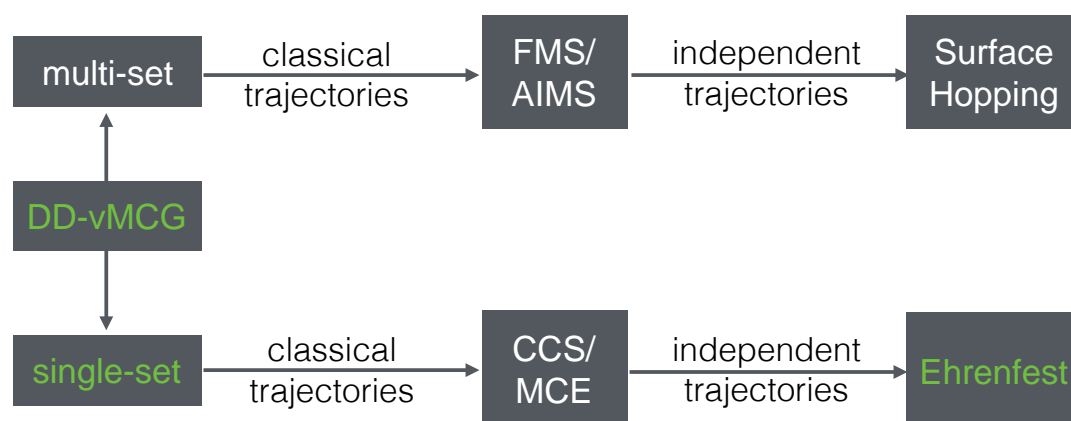

Figure 10: Schematic representation of the relationships among on-the-fly methods able to describe non-adiabatic dynamics [6]. DD-vMCG: direct dynamics variational multi-configurational Gaussian. FMS: full multiple apawning. AIMS: ab initio multiple spawning. CCS: coupled coherent state. MCE: multi-configurational Ehrenfest. In green are the methods used for simulations in my doctoral work.

Engineering coherent electron dynamics in molecules

Before discussing the consequences of including the nuclear coordinates in the treatment of coherent electron dynamics, a few remarks need to be made about the "oscillating motion" of the electronic density. These oscillations depends on the nature of the electronic eigenstates involved and may actually be visible or not. Let us take the example of electron dynamics induced upon valence ionisation of bismethylene-adamantane (BMA), a model donor-linker-acceptor system where there is an electron transfer between two π bonds connected by the adamantane framework. Vertical ionisation of the π system at the equilibrium geometry of the neutral species leads to an exact point of degeneracy between the ground and first excited states of the cation, i.e. no electron dynamics since the period of oscillations is inversely proportional to the energy and would therefore be infinite. One could imagine a chemical modification in order to lift the degeneracy and "engineer" electron dynamics. There exist in general two nuclear coordinates along which the electronic degeneracy is lifted to first order. In BMA, these are the antisymmetric stretching of the two π bonds and the deformation of the adamantane cage. A distortion along the former leads to the adiabatic ground state of the cation having the charge localised on one methylene bond while the adiabatic first excited state has the charge localised on the other methylene bond. A superposition of these two states would result in a delocalised hole over the two methylene groups and not in charge oscillations between spatially separated parts of the molecule (Figure 11, top). For coherent electron dynamics to be visible, the superposition of the two states needs to result in a hole localised on one methylene bond, i.e. the adiabatic states needs to be made of the delocalised holes with opposite phase (Figure 11, bottom). This is achieved in BMA by "chemically" deforming the adamantane cage, i.e. altering the number of carbon atoms in the rings forming the cage, for instance having four connected cyclopentane (instead of cyclohexane) rings [9]. Different chemical deformations of the adamantane cage result in different energy gaps between the cationic states and thus different periods of oscillations in the electronic density. This example illustrates the conditions necessary for the oscillating motion of the electronic density to be visible. An important point is that a non-zero energy gap is not a sufficient condition; the electronic character of the states matters. It also demonstrates how one can control the time scale of such coherent electron dynamics in molecules [9, 10, 11].
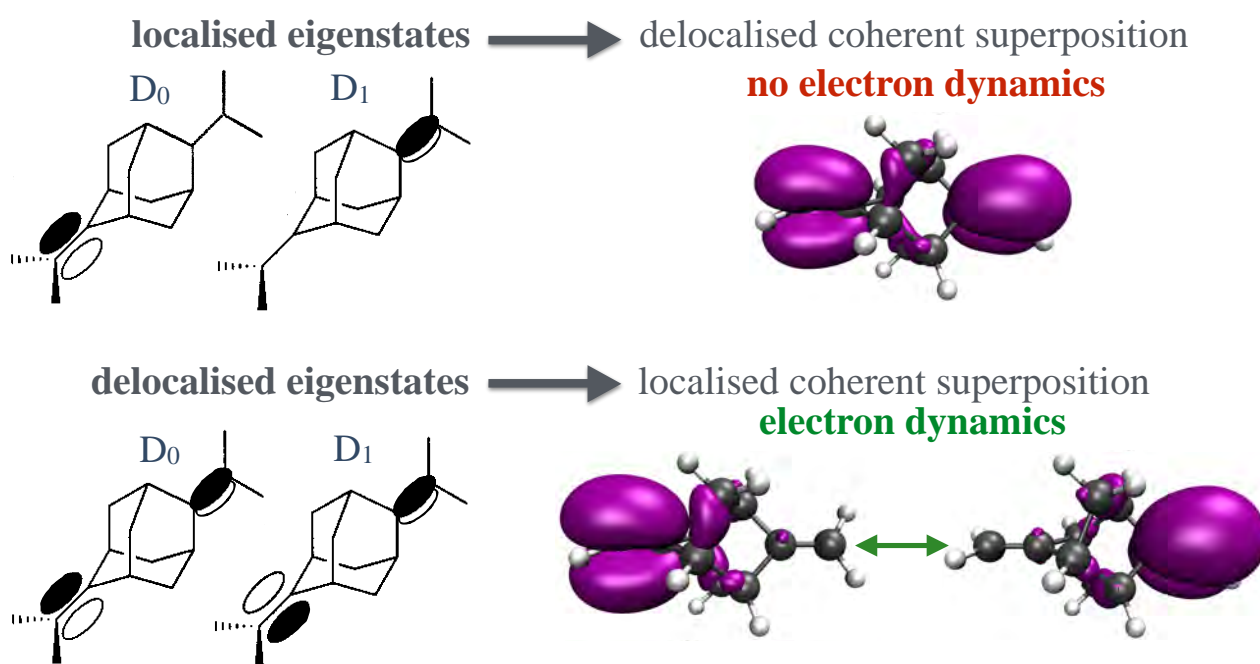

Figure 11: Engineering of coherent electron dynamics in molecules. An antisymmetric stretching of the two π bonds leads to localised electronic eigenstates and therefore a delocalised hole in the superposition i.e. no electron dynamics (top) while the deformation of the adamantane cage leads to delocalised eigenstates with opposite phase and therefore oscillations between the two methylene bonds [9] (bottom).

Effect of mean-field nuclear motion on coherent electron dynamics

One of the aims of my doctoral work has been to study the validity of the *fixed-nuclei approximation*, often used in simulations of molecular electron dynamics. The justification given for this approximation is the expected difference in time scales of electron and nuclear dynamics, the electron distribution changing much faster than the nuclear geometry. With the examples of toluene and para-xylene, I have aimed to understand further the extent to which neglecting nuclear motion is a reasonable approximation [10]. Vertical ionisation in these systems takes place at geometries near the degeneracy points between ground and first excited states of their cations. I have compared pure electron dynamics simulations (neglecting the nuclear degrees of freedom) with simulations of coupled electron and nuclear dynamics using the mean-field Ehrenfest method. To follow the evolution of the electronic wave packet, its spin density – that locates the unpaired electron – is computed and partitioned onto the atoms at each step of the simulation. The evolution of the partitioned spin densities with fixed nuclei and nuclei moving are shown on the left and right panels of Figure 12, respectively. One of the key findings of my research is that the nature and timescale of the oscillating motion in the electronic density can be affected by the nuclear motion, due to non-adiabatic relaxation and changes in the energy gap. The amplitude of these effects is system-dependent. In para-xylene, electron dynamics seems to be too fast for the nuclear motion to have a very significant effect on this timescale (Figures 12c and d). However, in toluene (where ionisation takes place closer to the electronic degeneracy in the cation), the effects are significant after only 2-3 fs (Figures 12a and b). Indeed, as the energy gap decreases, the electron dynamics slows down to the timescale of nuclear motion. There is then a strong interaction between the electronic and nuclear degrees of freedom. Importantly, the non-adiabatic relaxation of electronic population does not seem to lead to a significant electronic decoherence within the first tens of fs [12, 13].
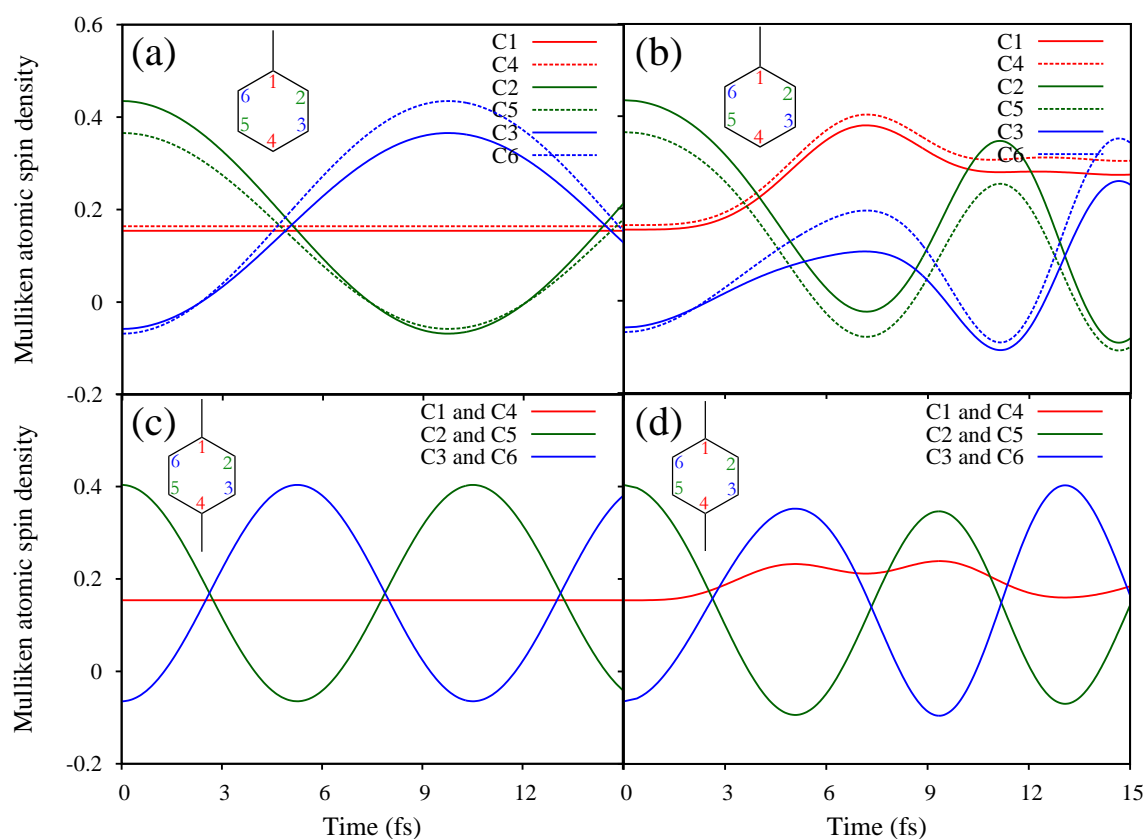

Figure 12: Effect of mean-field nuclear motion on coherent electron dynamics: Evolution of the spin densities partitioned onto the atoms after ionisation of toluene (a,b) and para-xylene (c,d) [10]. Simulations with fixed nuclei are on the left (a,c) and with nuclei moving according to the Ehrenfest method on the right (b,d).

Effect of nuclear spatial delocalisation on coherent electron dynamics

Another pupose of my doctoral work has been to study the effect of the natural width of the nuclear wave packet on electron dynamics (independently from the nuclear wave packet motion itself) neglected in the so-called *single-geometry approximation*. By using the Wigner distribution function – a quantum distribution function in classical phase space – to represent the delocalised nuclear wave packet, I have proposed a more realistic approach to describe electron dynamics in molecules. This led to one of the most significant advances in our field: because of the nuclear wavepacket delocalisation, oscillations in the electronic density dephase with time and overall electron dynamics disappears [14, 15, 9].

In the para-xylene cation, Figure 13a shows the electron dynamics – as in Figure 12c – for an ensemble of 500 nuclear geometries, simulated independently. The distribution of nuclear geometries leads to a distribution in energy gaps and therefore of oscillation periods in the electronic density (Figure 13b). A close look allows one to distinguish the individual oscillations (with different periods) that dephase with time (Figure 13a). The average oscillation amplitude is shown as a solid white line. We see a half oscillation reaching its turning point at about 3 fs, and then it goes to zero: The coherent electron dynamics quickly disappears with a half-life of about 4 fs. The dephasing is so fast that there is not even a single oscillation in the electronic spin density. The same conclusion holds with a nonequally weighted superposition (dashed white line), showing the robustness of these results with respect to the initial conditions. In this system, the effect of the nuclear wave packet width on electron dynamics is larger than the effect of the nuclear motion per se (Figure 12d).

I have also developed a simple analytical model which provides the general conditions for "longer-lived" electron dynamics: a narrow nuclear wave packet and almost parallel potential-energy surfaces of the states involved (Figure 13b). This enables the definition of molecular targets in which longer-lived coherent electron dynamics might be observed [14, 11].
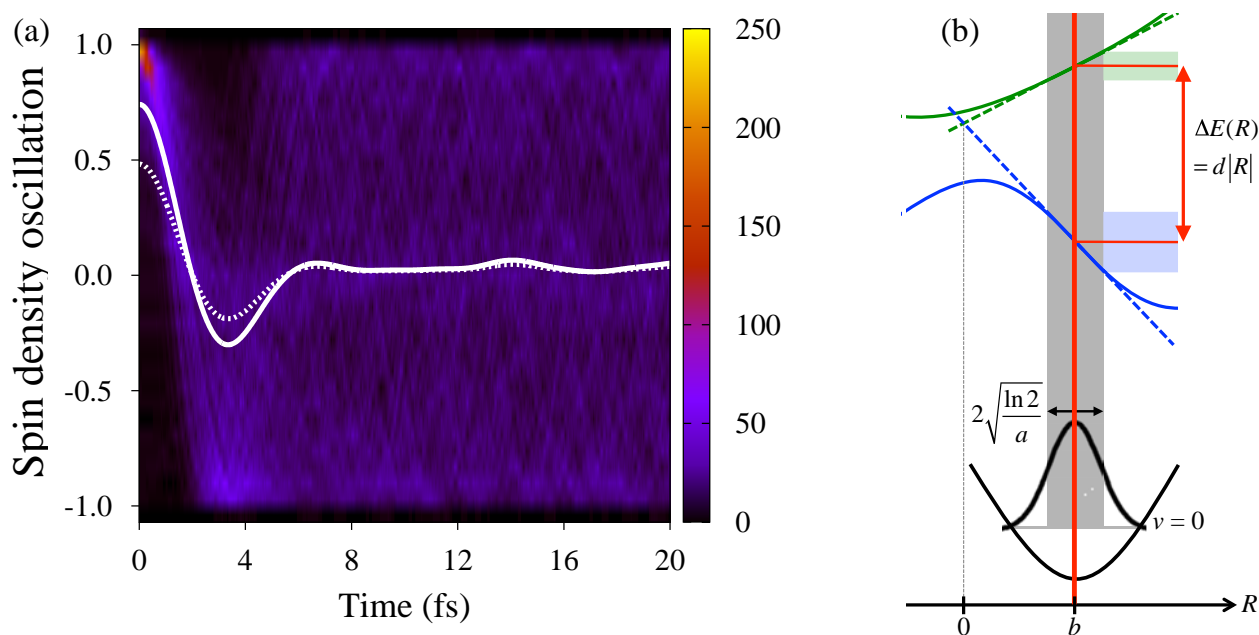

Figure 13: Effect of nuclear spatial delocalisation on coherent electron dynamics [14]: (a) Electron dynamics in para-xylene as in Figure 12c for an ensemble of 500 nuclear geometries reproducing the vibrational ground state before ionisation. The white lines represent the averaged electron dynamics for two different initial electronic populations. (b) Analytical model showing how the spatial delocalisation of the nuclear wave packet leads to a fast dephasing of the oscillations and providing the general conditions for longer-lived coherent electron dynamics.

Effect of quantum nuclear motion on coherent electron dynamics

The above results have shown that the (mean-field) nuclear motion treated classically with the Ehrenfest method affects but does not destroy coherent electron dynamics, while the intrinsic distribution of geometries in a nuclear wave packet leads to a fast dephasing of the oscillations in the electronic density. The latter prediction was obtained using an ensemble of independent trajectories. However, the effect of the nuclear motion may be underestimated with a mean-field approach and the quantum behaviour of the nuclei will not be described by independent trajectories. Also, these methods do not allow the nuclear wave packets on different electronic states to move in different ways, which may potentially lead to greater electronic decoherence. Here, I report an example of the modified bismethylene-adamantane BMA[5,5] cation (Figure 11) where the DD-vMCG method is used to simulate the effect of quantum nuclear motion on molecular coherent electron dynamics (including all decoherence mechanisms and all nuclear coordinates) [5]. These simulations were a major computational achievement, but also allowed us to gain new physical insights into the expected decoherence process that will impact on experimental as well as computational research. Figure 14a shows the oscillations in the electronic density: values around +1 corresponds to a hole density on the left double bond and values around -1 to a hole density on the right double bond (Figure 11, bottom). The oscillations are damped with time: electron dynamics decoheres such that the hole stays more delocalised over the two double bonds. A measure of the electronic coherence is plotted in Figure 14b (solid line): there is a fast electronic decoherence, exhibiting interesting structures, and reaching half the initial value at about 6 fs. These pioneering calculations using the fully quantum mechanical method confirm thus the very fast decoherence of electron dynamics on the time scale of a few femtoseconds, and also demonstrate the interplay of different mechanisms. The non-adiabatic relaxation of population has little effect on the time scale considered (Figure 14b, dotted line that stays equal to 1/2), consistently with the results of the previous section. The dephasing mechanism leads on its own to very fast decoherence (Figure 14b, dashed line). This result is in good agreement with the results obtained previously with an ensemble of fixed geometries sampled from the Wigner distribution [9]. The total decoherence can actually be slower; taking into account the nuclear overlap decay partially compensates for the very fast dephasing and gives rise to small coherence revivals. Our hypothesis to interpret this somewhat surprising result is the following: The decay of the GBF overlaps decreases the amplitude of the oscillations for some components of the wave packet, and thus the dephasing caused by these components will be less important, leaving on average a higher amplitude oscillation. In BMA[5,5], the two states have similar character, the difference in slopes is small and thus, the nuclear wave packets move only slightly away, limiting the effect of dephasing but still maintaining some significant overlap.
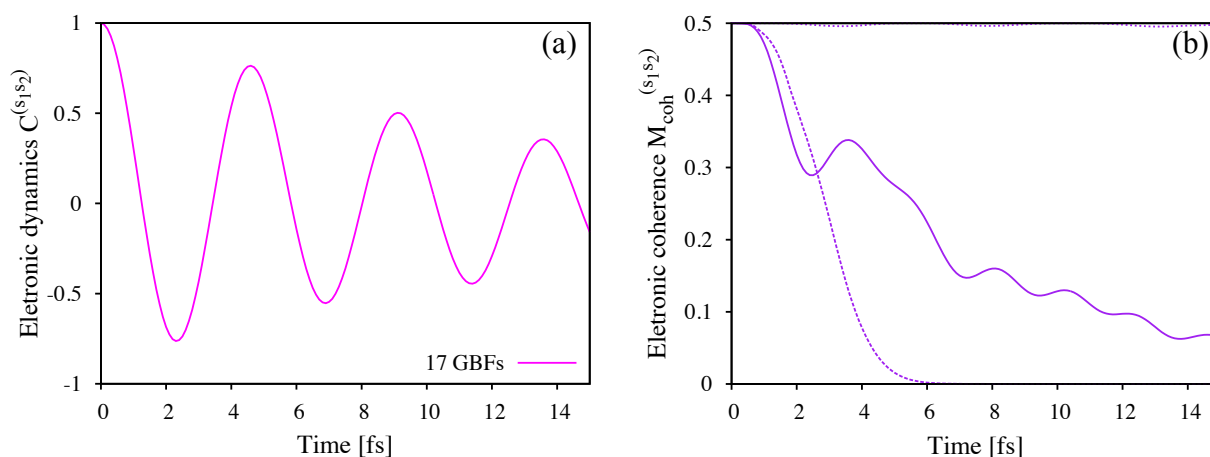

Figure 14: Electron dynamics coupled with quantum nuclear motion in BMA[5,5] [5]. (a) Coherent electronic oscillations in the electronic density, in simulations with 17 GBF. (b) Measure of electronic coherence (solid line), where the non-adiabatic relaxation mechanism (dotted line that stays mostly equal to 0.5) and dephasing mechanism (dashed line) are isolated.

Electronic coherent control of nuclear motion

A complementary aspect of the molecular coherent electron dynamics upon ionisation is the nuclear motion induced by the electronic wavepacket. The convenient picture of a single Born-Oppenheimer potential energy surface is lost and the nuclei "feel" the multiple coupled potential energy surfaces. Let us write the coherent superposition of two electronic states as $\Psi = \cos(\theta/2)\psi_0 + \sin(\theta/2)e^{i\phi}\psi_1$, where the mixing angle $\theta/2$ determines the relative weight of both electronic states, while ϕ expresses the relative phase between the two states. I have used the Bloch sphere to represent the coherent electronic wavepacket as a vector (Figure 15a). The projection of this vector onto the real plane can be interpreted as the nuclear gradient in the two nuclear coordinates of the branching space (Figure 15b) [16]. My results show how, by choosing the initial electronic state (relative weight $\theta/2$ and phase ϕ of the electronic wavepacket), one can control the initial nuclear motion, i.e. how much certain bond lengths are shortened or lengthened and how much of a shearing motion takes place (Figure 15c) [17]. Different superpositions of electronic states lead to different *effective* potential energy surfaces. Real-valued electronic wave packets induce nuclear motion of the same magnitude, with a direction in the branching space determined by the mixing angle. Considering complex-valued superpositions allows one to also control the velocity as well as the direction of nuclear dynamics in the branching space (Figure 15c). I have shown that the mean-field Ehrenfest method correctly predicts the average nuclear motion simulated with the full quantum mechanical method. However, I have found that the latter is necessary to provide the details of the nuclear dynamics on each electronic state. The relative weight and phase of a superposition can both be varied experimentally in principle, providing a route towards coherent electronic control of nuclear motion following ionisation.
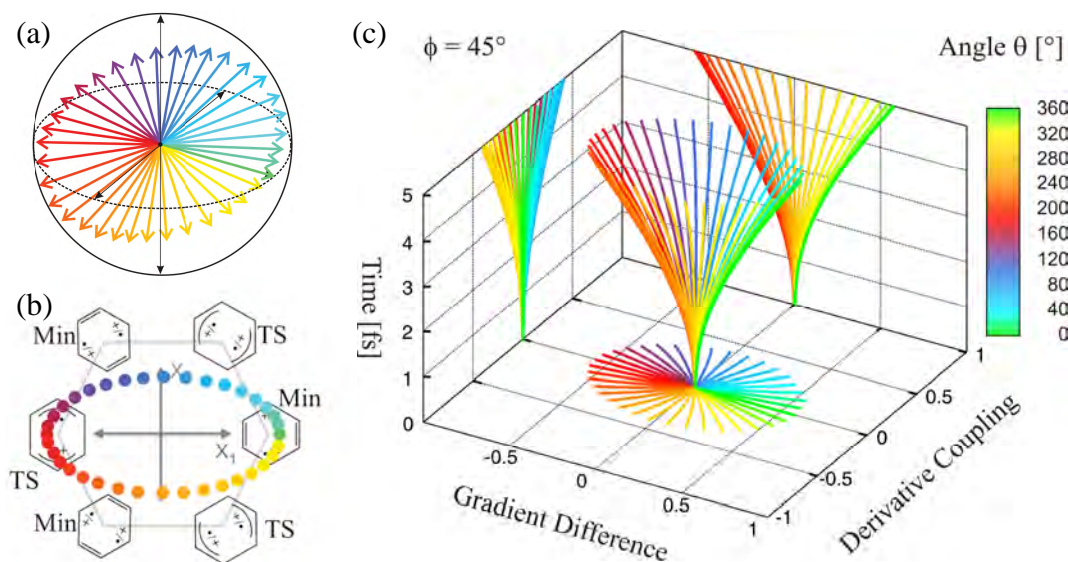

Figure 15: Electronic coherent control of nuclear motion [16]. (a) Representation of a set of different coherent electronic wave packets on a Bloch sphere. Here, a relative phase of $\phi = 45°$ was used while the mixing angle was systematically changed from $\theta = 0°$ to $350°$. (b) Diagram representing the projection of the Bloch vectors onto the real plane. (c) Corresponding Ehrenfest nuclear trajectories along the two nuclear coordinates of the branching plane.

Conclusion

In summary, we have learnt from specific examples that the nuclei can have important effects on the coherent electron dynamics following molecular ionisation. The different effects are common to all molecules and their significance will be system-dependent. A central and novel result of my thesis is that the simple picture of long-lived electron dynamics at a well-defined frequency predicted by the fixed-nuclei and single-geometry approximations does not

survive the coupling with the nuclear degrees of freedom. A fast damping of the oscillations is now expected. This is especially relevant for the experimental attempts to observe oscillations in the electronic density upon molecular ionisation.

References

[1] M. Hentschel, R. Kienberger, C. Spielmann, G. A. Reider, N. Milosevic, T. Brabec, P. Corkum, U. Heinzmann, M. Drescher, and F. Krausz, "Attosecond metrology," *Nature*, vol. 414, no. 6863, pp. 509–513, 2001.

[2] P. M. Paul, E. S. Toma, P. Breger, G. Mullot, F. Augé, P. Balcou, H. G. Muller, and P. Agostini, "Observation of a train of attosecond pulses from high harmonic generation," *Science*, vol. 292, no. 5522, pp. 1689–1692, 2001.

[3] A. I. Kuleff and L. S. Cederbaum, "Ultrafast correlation-driven electron dynamics," *Journal of Physics B: Atomic, Molecular and Optical Physics*, vol. 47, no. 12, p. 124002, 2014.

[4] F. Calegari, D. Ayuso, A. Trabattoni, L. Belshaw, S. De Camillis, S. Anumula, F. Frassetto, L. Poletto, A. Palacios, P. Decleva, J. B. Greenwood, F. Martín, and M. Nisoli, "Ultrafast electron dynamics in phenylalanine initiated by attosecond pulses," *Science*, vol. 346, no. 6207, pp. 336–339, 2014.

[5] M. Vacher, M. J. Bearpark, M. A. Robb, and J. a. P. Malhado, "Electron dynamics upon ionization of polyatomic molecules: Coupling to quantum nuclear motion and decoherence," *Physical Review Letters*, vol. 118, p. 083001, 2017.

[6] M. Vacher, M. J. Bearpark, and M. A. Robb, "Direct methods for non-adiabatic dynamics: connecting the single-set variational multi-configuration gaussian (vmcg) and ehrenfest perspectives," *Theoretical Chemistry Accounts*, vol. 135, no. 8, pp. 1–11, 2016.

[7] M. Vacher, D. Mendive-Tapia, M. Bearpark, and M. Robb, "The second-order ehrenfest method," *Theoretical Chemistry Accounts*, vol. 133, no. 7, p. 1505, 2014.

[8] K. Spinlove, M. Vacher, M. Bearpark, M. Robb, and G. Worth, "Using quantum dynamics simulations to follow the competition between charge migration and charge transfer in polyatomic molecules," *Chemical Physics*, vol. 482, pp. 52 – 63, 2017. (on the occasion of the 70th birthday of Lorenz S. Cederbaum).

[9] M. Vacher, F. E. A. Albertani, A. J. Jenkins, I. Polyak, M. J. Bearpark, and M. A. Robb, "Electron and nuclear dynamics following ionisation of modified bismethylene-adamantane," *Faraday Discussions*, vol. 194, pp. 95–115, 2016.

[10] M. Vacher, D. Mendive-Tapia, M. J. Bearpark, and M. A. Robb, "Electron dynamics upon ionization: Control of the timescale through chemical substitution and effect of nuclear motion," *The Journal of Chemical Physics*, vol. 142, no. 9, p. 094105, 2015.

[11] A. J. Jenkins, M. Vacher, R. M. Twiddle, M. J. Bearpark, and M. A. Robb, "Charge migration in polycyclic norbornadiene cations: Winning the race against decoherence," *The Journal of Chemical Physics*, vol. 145, no. 16, 2016.

[12] D. Mendive-Tapia, M. Vacher, M. J. Bearpark, and M. A. Robb, "Coupled electron-nuclear dynamics: Charge migration and charge transfer initiated near a conical intersection," *The Journal of Chemical Physics*, vol. 139, no. 4, p. 044110, 2013.

[13] M. Vacher, M. J. Bearpark, and M. A. Robb, "Communication: Oscillating charge migration between lone pairs persists without significant interaction with nuclear motion in the glycine and gly-gly-nh-ch3 radical cations," *The Journal of Chemical Physics*, vol. 140, no. 20, p. 201102, 2014.

[14] M. Vacher, L. Steinberg, A. J. Jenkins, M. J. Bearpark, and M. A. Robb, "Electron dynamics following photoionization: Decoherence due to the nuclear-wave-packet width," *Physical Review A*, vol. 92, p. 040502, 2015.

[15] A. J. Jenkins, M. Vacher, M. J. Bearpark, and M. A. Robb, "Nuclear spatial delocalization silences electron density oscillations in 2-phenyl-ethyl-amine (pea) and 2-phenylethyl-n,n-dimethylamine (penna) cations," *The Journal of Chemical Physics*, vol. 144, no. 10, 2016.

[16] J. Meisner, M. Vacher, M. J. Bearpark, and M. A. Robb, "Geometric rotation of the nuclear gradient at a conical intersection: Extension to complex rotation of diabatic states," *Journal of Chemical Theory and Computation*, vol. 11, no. 7, pp. 3115–3122, 2015.

[17] M. Vacher, J. Meisner, D. Mendive-Tapia, M. J. Bearpark, and M. A. Robb, "Electronic control of initial nuclear dynamics adjacent to a conical intersection," *The Journal of Physical Chemistry A*, vol. 119, no. 21, pp. 5165–5172, 2015.

Computational Physics Group News

- ## The Computational Physics Annual PhD Thesis Prize

    Each year, the IoP Computational Physics Group awards a Thesis Prize to the author of the PhD thesis that, in the opinion of the Committee, contributes most strongly to the advancement of computational physics.

    The winner of this year's Thesis Prize is Ioan Magdau for his thesis entitled "Theoretical Investigation of Solid Hydrogen and Deuterium", which was undertaken at the University of Edinburgh.

    Runner-up prizes are awarded to Morgane Vacher, for her thesis entitled "Electron and Nuclear Dynamics Following Molecular Ionization: Computational Methods and Applications", carried out at Imperial College London and Ahmed Al-Refaei, for his thesis entitled "Efficient Production of Hot Molecular Line List", carried out at UCL.

    Thanks to the generosity of AWE (`http://www.awe.co.uk`) Ioan receives £300 and Ahmed and Morgane receive £100 each for their achievements. Details of Ioan and Morgane's work are reported in this issue, and Ahmed's work will be reported in a forthcoming issue of the group newsletter.

    The deadline for applications of the 2018 prize is 30th April and details are available at the following link: `http://www.iop.org/activity/groups/subject/comp/prize/page_40691.html`

    Applications are encouraged across the entire spectrum of computational physics. Entry is open to all students from an institution in the UK or Ireland, whose PhD examination has taken place since 1st January 2017 and up to the submission deadline, and who did not apply for the CPG Thesis Prize in the previous year. Prize winners will be invited to write a feature article in the Computational Physics Group newsletter.

    Candidates are asked to note that if a similar thesis prize is offered by another IOP group (such as the Theory of Condensed Matter group), the Committee intends to liaise with that group so that both prizes will not be awarded to the same applicant.
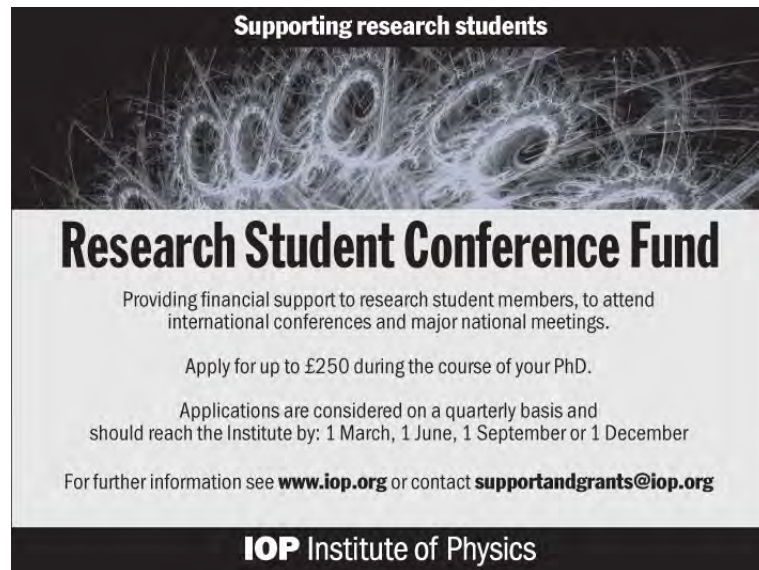
    The submission format is as follows:

    - A four page (A4) abstract describing the background and main achievements of the work
    - A one page (A4) citation from the PhD supervisor
    - A one page (A4) confidential report from the external thesis examiner

    Entries (PDF documents preferred) should be submitted by email, with "IOP CPG Thesis Prize" as the subject header, to Dr Arash Mostofi (a.mostofi@imperial.ac.uk). Any queries should also be directed to Dr Arash Mostofi. A few more details, including a list of past winners, can be found on the group webpage `http://www.iop.org/activity/groups/subject/comp/prize/page_40691.html`.

- **IoP Computational Physics Group - Research Student Conference Fund**

The Institute of Physics Computational Physics Group is pleased to invite requests for partial financial support towards the cost of attending scientific meetings relevant to the Group's scope of activity. The aim of the scheme is to help stimulate the career development of young scientists working in computational physics to become future leaders in the field.

Further details on this award can be found at:

`www.iop.org/activity/groups/subject/comp/prize/page_40691.html`

Conference and Workshop reports

- ## Conference on Computational Optical Sensing and Imaging, part of Imaging and Applied optics congress 2017

  26-29 June 2017, San Francisco, California, United States

  Highlights. The IOP computational imaging group awarded me £150 to travel to San Francisco to attend the OSA Imaging and Applied Optics Congress, and present a poster at the Computational and Optical Sensing and Imaging (COSI) session. I am a first year PhD student in the imaging concepts group at the University of Glasgow, headed by Professor Andrew Harvey. My PhD project is entitled Computational Imaging and is being undertaken in partnership with the North Wales based company Qioptiq. The Congress has several sessions, in which COSI was just one, which allowed me to pick and choose talks to attend and allowed for an overview of several areas in computational imaging simultaneously. A significant presence at the conference was Laura Wallers group from Berkley, with an emphasis on presenting lensless imaging technologies (specifically Grace Kuo and Nick Antipa), in both 3D and 2D settings respectively. This was starkly offset by the fantastic talk by David Brady (Duke University) which had an emphasis on lenses being an integral and irreplaceable part of the imaging system. Light Field imaging was also a heavily used term, where Laura Waller, again, delivered a very interesting talk on utilising the Wigner function applied to single shot light field images. This development from the standard plenoptic function that is used to decipher like-light field images allowed her to undertake single shot 3D neural activity tracking. The Light Field imaging and Display Systems Tutorial, held by Nikil Balram was also very enlightening and facilitated and application based discussion about the future of the field. I thoroughly enjoyed my first international conference and feel very lucky to have been allowed this opportunity so early within my PhD. I think the experience was invaluable and has inspired me to work harder at this early stage in my career. I spoke to leaders in my field and my contemporaries, PhD students at similar stages to myself, drawing on their experiences and sharing my own âĂŞ the early stages of networking. For me the conference was very successful, holding 5 sessions simultaneously in the same imaging congress allowed for diversity of conference attendees and of subject areas. San Francisco is also a very good choice of city for a conference as traditionally it creates an atmosphere for dynamic discussion, while simultaneously being a hotbed for innovation. COSI was a valuable first international conference, it was not too large that the experience was overwhelming, however there were enough people linked to the field of computational imaging for it to be very worthwhile.

  Report kindly provided by Laura Cowan, PhD student, School of Physics and Astronomy at University of Glasgow

- ## Sol-SkyMag 2017, 19th June - 23rd June

  19th June - 23rd June in San Sebastian (Gipuzkoa), Spain

  Highlights. The San Sebastian campus of Euskal Herriko Unibertsitatea (EHU), in the Basque Country in Spain, recently hosted the 2nd Annual Sol-SkyMag conference. It was attended by leading researchers working in both experimental and theoretical magnetism, and focused mainly on solitons and skyrmions in magnetic systems. The conference attracted around 80 international researchers, with a large number of delegates from research groups in Russia, Germany and Spain, and was organised and chaired by Prof. Konstantin Guslienko of EHU.

  After a short introductory reception on the evening of the 19th June, the main part of the conference started on the 20th with a plenary talk covering the current research on magnetic skyrmions, which was presented by Professor Albert Fert, winner of the 2007 Nobel Prize in Physics for his part in the discovery of Giant

Magnetoresistance. This enlightening talk gave an overview of current experimental and theoretical work, and covered the production of, imaging of and manipulation of skyrmions. Following this, over the course of the four days of the conference were a number of sessions of invited and contributed talks, and a poster session. Many of the talks covered computational research in the field, and a particularly impressive talk was given by Dr Felipe Rybakov, in which he showed a live demonstration of atomistic spin dynamics simulations in order to emphasise certain behaviour of skyrmions.

While at the conference, I gained a lot by discussing work with other attendees, particularly during the poster session, and I felt that this opportunity gave me knowledge of the broader context in which to set my own research in future. The conference itself was particularly successful at bringing together the experimental and theoretical communities who research skyrmions. I would like to thank the Computational Physics Group for the bursary which has allowed me to attend the conference.

Report kindly provided by Ryan Pepper, PhD student, Computational Modelling Group at University of Southampton

Upcoming Events of Interest

Upcoming events of interest to our readers can now be found via the following web links.

- IOP's index page for scientific meetings, including conferences, group events and international workshops:

    `www.iop.org/events/scientific/index.html`

- IOP Conferences page for conference information, calendar and noticeboard:

    `www.iop.org/events/scientific/conferences/index.html`

- All events being run or supported by IOP Groups including calendar and links to event web pages:

    `www.iop.org/events/scientific/group/index.html`

- Thomas Young Centre: The London Centre for Theory and Simulation of Materials organises many different kinds of scientific events on the theory and simulation of materials, including Highlight Seminars, Soirees and Workshops. For further details of upcoming events please visit:

    `www.thomasyoungcentre.org/events/`

- CECAM is a European organization devoted to the promotion of fundamental research on advanced computational methods for atomistic and molecular simulation and their application to important problems in science and technology. CECAM organises a series of scientific workshops, tutorials and meetings. For further details please visit:

    `www.cecam.org`

Computational Physics Group Committee

The current members of the IoP Computational Physics Group committee with their contact details are as follows:

Anton Shterenlikht (Chair)	mexas@bris.ac.uk
Arash Mostofi (Thesis prize)	a.mostofi@imperial.ac.uk
Bart Vorselaars (CPG blog)	bvorselaars@lincoln.ac.uk
Gavin Tabor (membership secretary)	g.r.tabor@ex.ac.uk
James Uhomoibhi (Secretary)	j.uhomoibhi@ulster.ac.uk
Jonathan Smith	jdasmith@gmail.com
Manuela Mura	mmura@lincoln.ac.uk
Marco Pinna (Newsletter and Treasurer)	mpinna@lincoln.ac.uk
Nicholas Chancellor (publicity secretary)	nicholas.chancellor@gmail.com
Nick Parker	nick.parker@ncl.ac.uk
Nikolaos Fytas	ab5298@coventry.ac.uk
Sally Bridgwater	sally.bridgwater@nag.co.uk
Simon Richards	s.richards@physics.org
Stephen Hughes	Stephen.Hughes@awe.co.uk

Some useful web links related to the Computational Physics Group are:

- CPG webpages
  `comp.iop.org`

- CPG Newsletters
  Current issue:
  `www.iop.org/activity/groups/subject/comp/news/page_40572.html`
  Previous issues:
  `www.iop.org/activity/groups/subject/comp/news/archive/page_53142.html`
  `www.soton.ac.uk/~fangohr/iop_cpg.html`

Related Newsletters and Useful Websites

The Computational Physics Group works together with other UK and overseas computational physics groups. We list their newsletter locations and other useful websites here:

- Newsletter of the Computational Physics Division of the American Physical Society:
  `www.aps.org/units/dcomp/newsletters/index.cfm`

- Europhysicsnews newsletter of the European Physical Society (EPS):
  `www.europhysicsnews.org/`

- Newsletter of the Psi-k (Ψ_k) network:
  `www.psi-k.org/newsletters.shtml`

- Computational Physics Group blog (CPG):
  `compphysics.org`